



LIGO Laboratory / LIGO Scientific Collaboration

LIGO-T1000090-v3

LIGO

March 25, 2010

advanced LIGO baffle design using SIS

Hiro Yamamoto

Distribution of this document:
LIGO Science Collaboration

This is an internal working note
of the LIGO Project.

California Institute of Technology
LIGO Project – MS 18-34
1200 E. California Blvd.
Pasadena, CA 91125
Phone (626) 395-2129
Fax (626) 304-9834
E-mail: info@ligo.caltech.edu

Massachusetts Institute of Technology
LIGO Project – NW17-161
175 Albany St
Cambridge, MA 02139
Phone (617) 253-4824
Fax (617) 253-7014
E-mail: info@ligo.mit.edu

LIGO Hanford Observatory
P.O. Box 1970
Mail Stop S9-02
Richland WA 99352
Phone 509-372-8106
Fax 509-372-8137

LIGO Livingston Observatory
P.O. Box 940
Livingston, LA 70754
Phone 225-686-3100
Fax 225-686-7189

<http://www.ligo.caltech.edu/>

1. Introduction

The size of baffles placed in front of the BS (beam splitter) to block the tail of the field from the ITM (input test mass) was calculated using a FFT-based simulation tool SIS^[1] (Stationary Interferometer Simulation). The design is based to reduce the asymmetry resulted from the finite size of the BS mirror and to minimize the loss of the signal sideband.

An optimal baffle size comes out to be an oval shape with axis sizes of 21cm x 26cm.

The effect of misplacement of baffles is discussed quantitatively.

2. Geometry of optical system

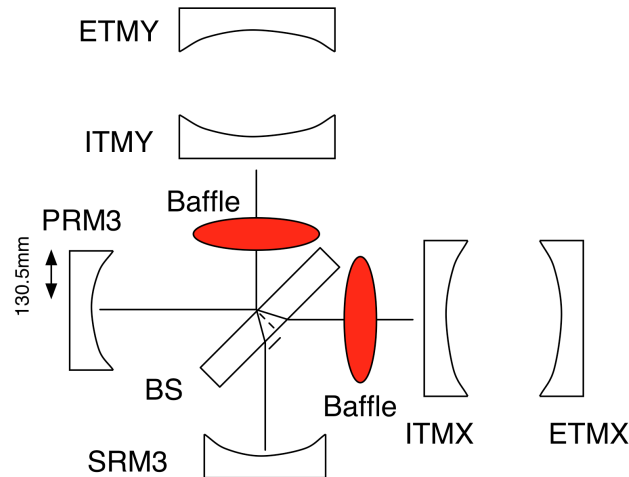


Figure 1 Optical configuration

Figure 1 shows the configuration of the aLIGO core optical system. Two additional mirrors are connected to each RM3 to form a power and a signal recycling cavity. The beam shape coming from the long arm is larger than the BS size in the plane of the IFO because the BS is rotated by 45° , and two baffles shown by red ovals are placed in front of the BS to shield these beams not to hit the suspension cage of the BS.

The term “beam shape” is used to mean the area where the beam has finite energy. When a beam is reflected by or goes through an optic, the beam shape after the interaction is the size of the reflecting side of the mirror or is the size of the clear aperture of the lens. Due to diffraction, the beam shape becomes larger through propagation in cavities than the well defined shape of the optic with which the beam last interacted. The simulation calculates the diffraction effect, but all qualitative discussions here neglect the change of the beam shape for simplicity. This is a good approximation in the cavity shown in Figure 1 where all propagations are near field propagation, i.e., cavity lengths, ~ 10 m, are all shorter than the Rayleigh range, ~ 1 km.

Figure 2 shows the geometry of the BS and beam shape interacting with the BS. Thick red lines, [A], [B], [C] and [D], show the center of beams coming from and going to PRM3, ITMY, ITMX

and SRM3. Depending on the direction of the interaction with the BS, each beam is affected differently by the finite size of the BS.

E.g., the beam from PRM3, whose size is 261mm, interacts with the full BS HR surface, (beam boundaries are [1] and [5] with the beam center [A], which is quoted as BB[5,A,1] here after). When it is reflected toward the ITMY, the full beam is reflected without loss, BB[2,B,6]. When it goes through the BS and goes toward the ITMX, part of the incoming beam cannot go through the BS, and the beam shape becomes asymmetric, BB[7,C,11].

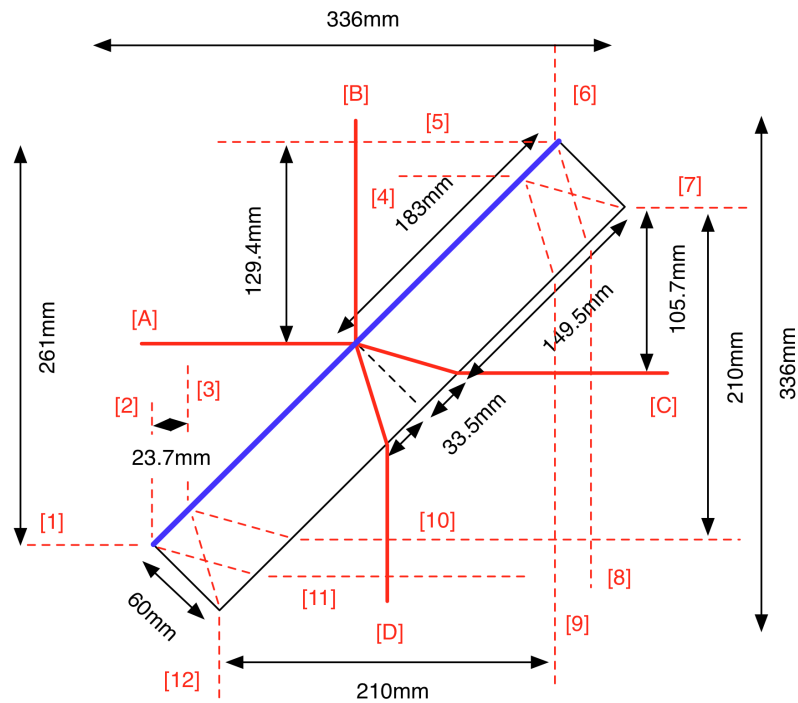


Figure 2 Beam Splitter geometry in the plane of the interferometer

The largest beam shape leaving BS is a circle with aperture 26cm, which is determined by the XRM3 aperture. The smallest one is an oval with axis sizes 26cm (out of IFO plane, y axis) and 21cm (in IFO plane, x axis). The axis size along y direction is determined by XRM3, while the axis size in the x plan is determined by the 45° rotated BS size and the BS thickness.

Figure 3 shows various beam shapes. The red circle is the ITM aperture size, and is larger than the beam shape going to the ITM from the BS, whose boundary is either blue or green, depending on the path going through or reflected by BS. Whatever the beam shape going to the ITM is, the resonating field in the arm cavity becomes a Gaussian field spreading to the edge of the test mass, and the beam shape coming out of the arm becomes the red circle shown in the figure. This mismatch of beam shapes introduces non-smooth structure in the field reflected by the ITM, which is discussed in the following section.

The radius of the cyan circle is twice of the beam size on the ITM, i.e., 5.3cm x 2. The power out of twice of the beam size, w , is $\exp(-8) \sim 340\text{ppm}$.

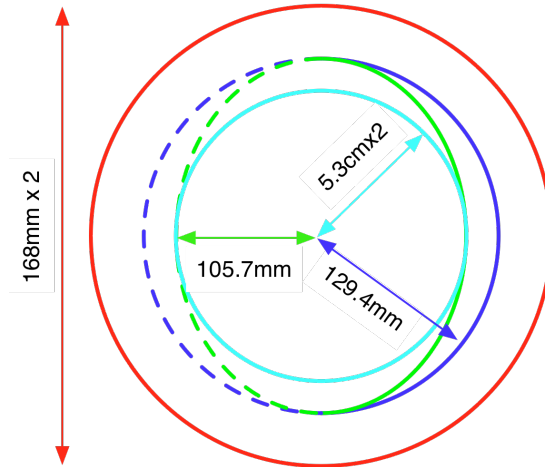


Figure 3 Beam shape

3. Simulation

A FFT based simulation code, SIS, was used for this analysis. The version used for this study simulated only a coupled cavity with a BS (CC), i.e., a coupled cavity of stable power recycling cavity (PRC) or a stable signal recycling cavity (SRC) and the X arm or Y arm with a BS placed between the ITM and the RM3. The BS has a wedge angle of 0.04° , and RM2 and RM3 have finite angle of incidence (AOI) for the unfolded IFO. Because of this limitation, the interference of the two fields, like the field in the dark port side of the BS, cannot be calculated precisely.

Figure 4 is an example of the field going from ITMX to BS in a coupled cavity formed by PRC and X arm. This is a log plot of the power in the x plane. The horizontal axis is x^2 times signal of x, so the shape is a straight line if the power distribution is Gaussian.

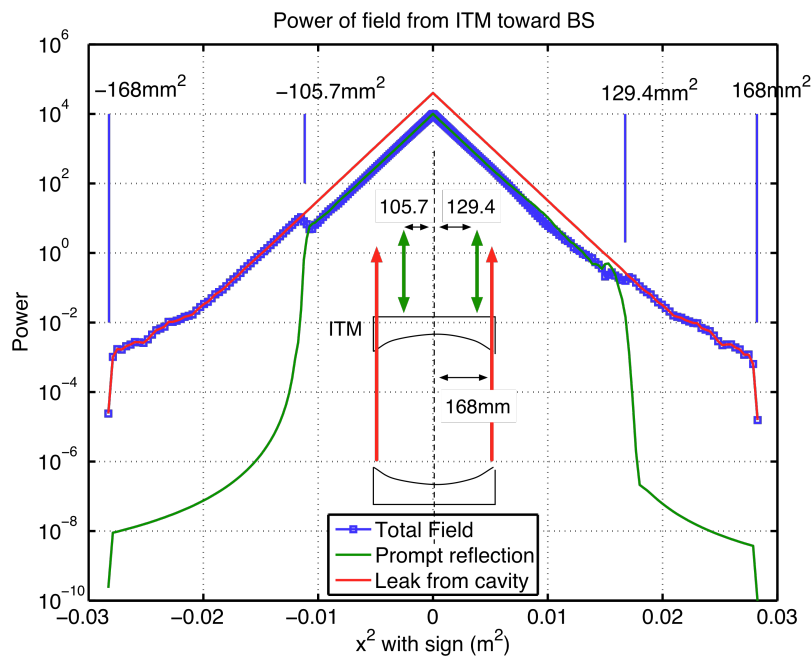


Figure 4 Field from ITM to BS in PRC-X arm cavity

The red line is the field coming out of the cavity, which is symmetric in x and extends up to the ITM aperture boundary. The green line is the promptly reflected field by the ITM. The beam boundary going to ITMX is BB[7,C,11] in Figure 2, and is not symmetric in the x distribution. The green line in Figure 4 is the reflection of this field and carries over the characteristics of the field going to ITM, i.e., one side ends at 10.5cm and the other side at 13cm.

The total reflected field, blue line, is the sum of the two fields, the leak field from the arm, red line, and the promptly reflected field, green line. For the CR field resonating in the arm, the leak field amplitude is -2 times the input field and the promptly reflected one is +1 times the input field, thus the total reflection is -1 times the input field. Because the input field is limited to the boundary at 10.5cm and at 13cm, the power of the reflected field goes up outside of these boundaries where the input field is 0.

Figure 5 is a similar plot, power distributions of fields on BS coming from ITMX and ITMY in four different coupled cavity configurations. The left plot shows distributions in the x axis, the plane of the IFO, while the right one in the y axis, out of the IFO plane.

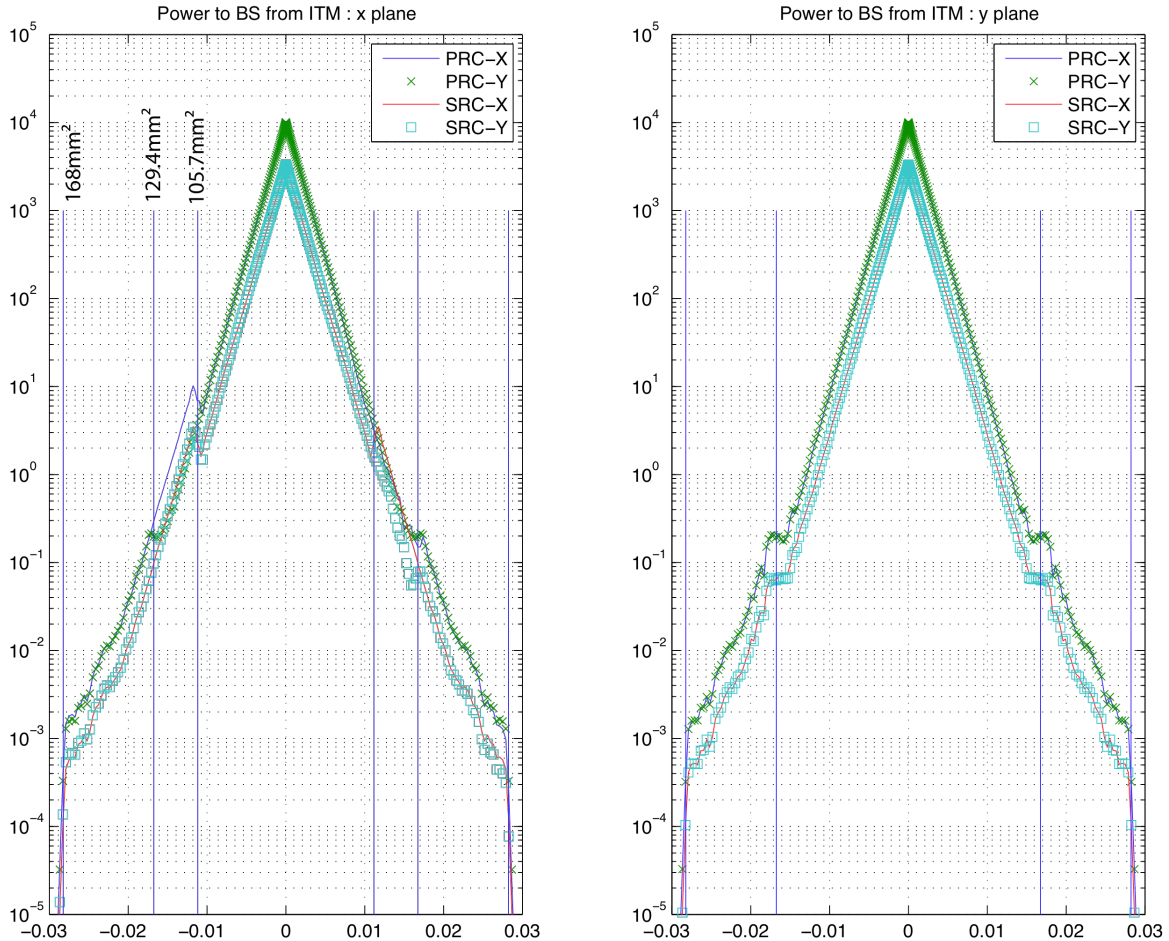


Figure 5 Fields on BS from ITM in four CC configurations

For each case, stationary fields are calculated by injecting a field with 1W power to the RM whose mode matches with the mode defined by the idealistic cavity, i.e., all optics have infinite apertures, the wedge angle of the BS and the AOI on RM2 and RM3 are 0.

In the y distribution, all 4 cases show symmetric distributions with jumps at 13cm radius. In the x distribution, distributions are different because each configuration has different clear aperture.

The power distribution in a cavity formed by the SRC and X arm (SRC-X) has jumps at radius $\pm 10.5\text{cm}$ because the beam going to ITMX is BB[7,C,10] in Figure 2, or the clear aperture of this transmission between SRC and ITMX is a pair of solid and dashed green lines in Figure 3. The clear aperture in SRC-Y is BB[6,B,3] in Figure 2, or a solid blue and dashed green lines in Figure 3.

4. Baffle design

In order to minimize the difference of beam shapes among fields contributing to the same port of the BS, and to make the beam shape symmetric in the x axis, a baffle was placed in the simulation whose shape is an oval with axis size 21cm (x axis) x 26cm (y axis). This corresponds to the pair of solid and dashed green lines in Figure 3.

Figure 6 shows fields on the BS going to RM3 with and without baffles. The top figure shows fields in a coupled cavity with PRC and the bottom one with SRC.

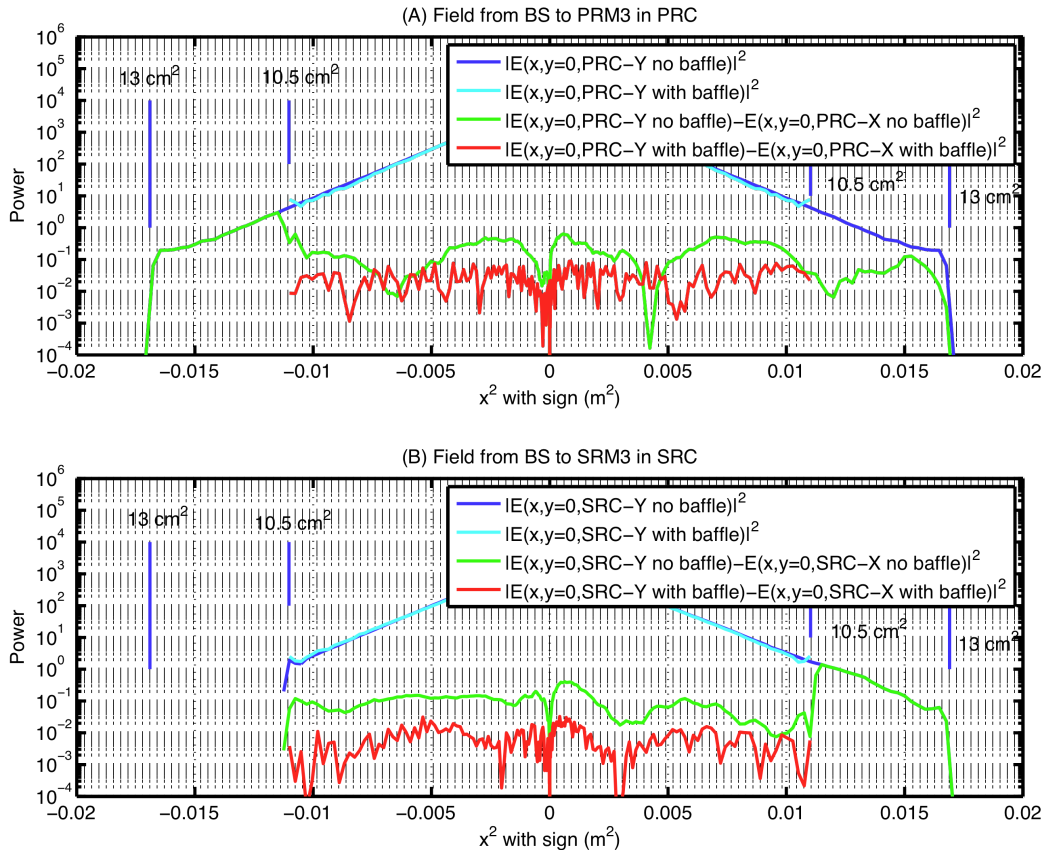


Figure 6 Field from BS to RM3 with and without Baffle

The solid blue lines show the power in a CC without baffle and the cyan lines show the power in a CC with baffle placed between the BS and the ITM. The green and red lines show the difference of fields (ΔE defined below) of PRC-X and PRC-Y in Figure(A) and the difference of SRC-X and SRC-Y in Figure(B).

$$\Delta E(x, y : RC) = E(x, y : RC - Yarm) - C \cdot E(x, y : RC - Xarm)$$

$$C \equiv E(0, 0 : RC - Yarm) / E(0, 0 : RC - Xarm)$$

$E(x, y : \text{PRC}/\text{SRC}-\text{Xarm}/\text{Yarm})$ is the field distribution on the BS going to RM3 in a coupled cavity formed by PRC or SRC and by X arm or Y arm with a BS in between. When calculating the difference, one is scaled by the ratio of the fields at the origin, i.e., $\Delta E(0, 0) = 0$. This scaling is done to estimate the imbalance of fields caused by this BS size effect and by the baffle.

The green lines are the case without baffles and the red ones are the case with baffles. By placing the baffle, the field coming out from the BS toward RM3 becomes more symmetric and the difference of fields in RC-X and RC-Y cavities becomes smaller.

	PRC	SRC
Without baffle	116	166
With baffle	22	21

Table 1 Contrast defect in ppm

Table 1 shows the ratio of the power of the field ΔE defined above and the power of $E(\text{RC}-\text{Yarm})$.

$$CD \equiv \frac{\int dx dy |\Delta E(x, y : RC)|^2}{\int dx dy |\Delta E(x, y : RC - Yarm)|^2}$$

As can be seen from this table, the mismatch of the fields in RC-X and RC-Y caused by the finite size of the BS optic is reduced by factor 5 or more by placing the baffle with the size of 21cm x 26cm.

The effect of the baffle on the signal sideband loss was found to negligible by the following calculation. The signal sideband is generated by oscillating the ETM at frequencies between 0 to 1kHz, and calculated the stationary field in SRC-X and SRC-Y cavities with and without baffles. The power of the TEM00 mode at each signal sideband frequency was calculated on the SRM.

This power of the signal sideband normalized by the CR power in the arm is the measure of the signal efficiency. The loss by placing the baffle between the BS and the ITM turns out to be completely negligible.

5. Effect of baffle misplacement

When a baffle is misplaced, the contrast defect will become larger. This effect was estimated by comparing fields in a SRC-Y cavity with different offset of the center of the baffle. For this study, difference of fields, δE , is introduced:

$$\delta E(x, y : dBX, dBY) = E(x, y : dBX, dBY) - E(x, y : dBX = 0, dBY = 0)$$

where dBX (dBY) is the offset of the center of the baffle along the x (y) axis.

The blue line in the top plot in Figure 7 shows the power distribution of the field on the BS going to SRM3. The green line shows $\delta E(x,0;2\text{mm},0)$. The bottom plot shows the power of this difference in the x-y plane, perpendicular to the beam propagation direction.

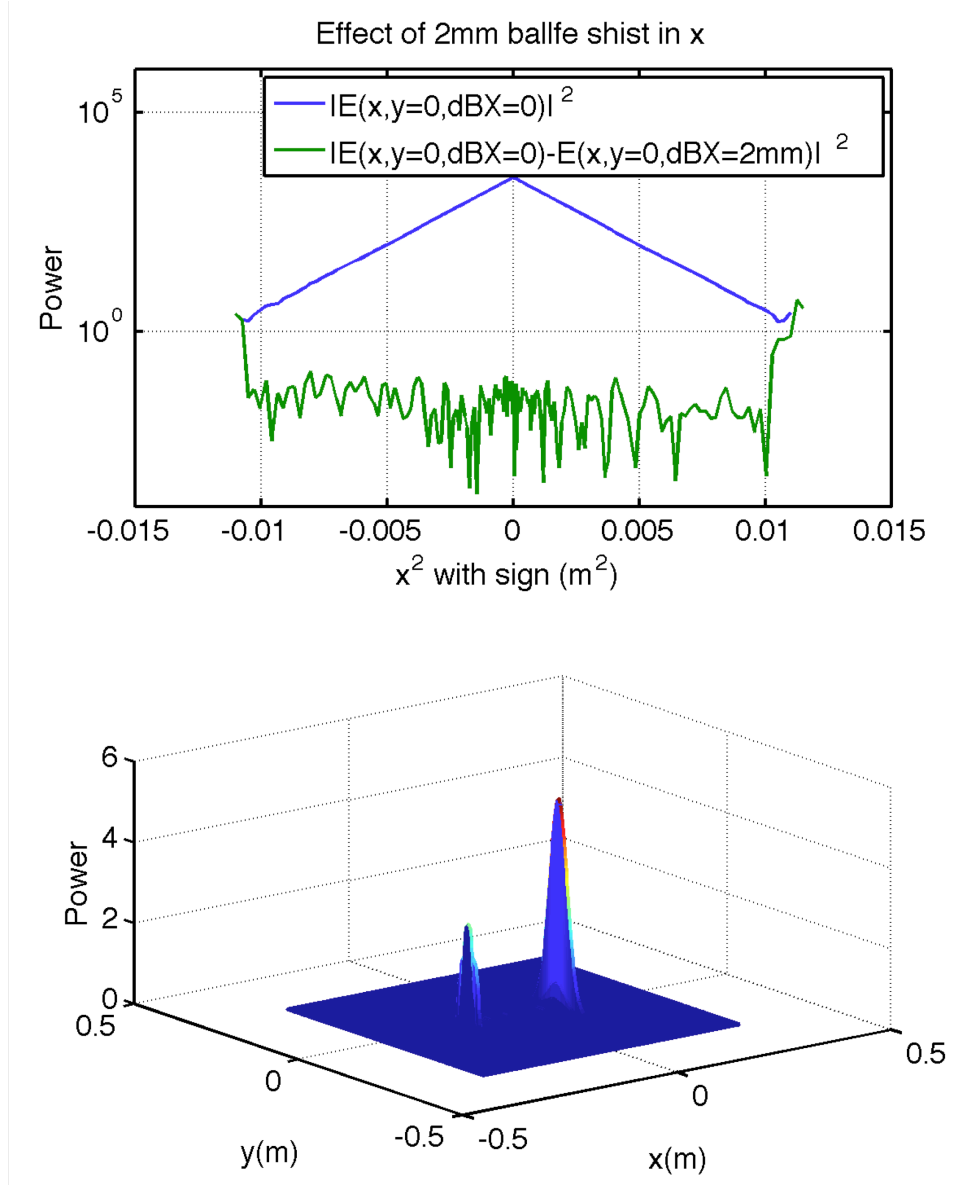


Figure 7 Contrast defect by misplacement of baffle

The increase of the contrast defect due to this misplacement defined as

$$dCD = \frac{\int dx dy |\delta E(x,y : offset, 0)|^2}{\int dx dy |E(x,y : 0, 0)|^2}$$

is summarized in the following table.

offset	0.5mm	1mm	2mm
dCD	18ppm	49ppm	101ppm

Table 2 Increase of contrast defect by misplacement of baffle

The displacement of the baffle in the x direction corresponds to the shift of the pair of green lines, solid and dashed, in the horizontal direction. The change of the field power which goes through this clear aperture can be approximately calculated as

$$\begin{aligned}\delta P(r, \delta) &= \frac{2}{\pi w^2} \left(\int_{-\infty}^{\infty} dy \int_{-r+\delta}^{r+\delta} dx - \int_{-\infty}^{\infty} dy \int_{-r}^r dx \right) \exp\left(-2 \frac{x^2 + y^2}{w^2}\right) \\ &\approx 2\sqrt{2} \exp\left(-2 \frac{r^2}{w^2}\right) \frac{\delta}{w}\end{aligned}$$

The size of the baffle in the horizontal direction is roughly twice of the beam size, and this change becomes 18ppm for 1mm displacement. The numerical result in the above table is consistent with this naive estimation of the baffle displacement effect.

The misplacement of the baffle in the y direction does not introduce any change of the contrast defect, because the baffle in that direction is large and the displacement of the baffle in that direction does not exclude or include any measurable energy.

6. Common mode rejection factor and various alternatives

The common mode rejection factor is calculated using the following expression.

$$C_{rej} = \left| \frac{a_{00}^x - a_{00}^y}{a_{00}^x + a_{00}^y} \right|$$

$$a_{00}^{x,y} = \frac{|TEM00(BS \rightarrow RM3)|}{\sqrt{Power(ITM \rightarrow ETM)}} \text{ (in SRC - X / Yarm)}$$

TEM00(BS->RM3) is the amplitude of the TEM00 mode of the signal sideband at 0 Hz going from BS toward RM3 in the coupled cavity formed by SRC and X or Y arm with BS in between. The source field in the arm is proportional to the store power in the arm, and $a^{x,y}$ is defined to be the TEM00 amplitude normalized by the arm power to suppress the small difference of the power in the arm in two coupled cavity setups.

The following table compares rejection factor for various configurations : difference baffle design and different BS and SRM3 sizes. Values for “4mm offset” are calculated by placing one baffle (either in SRC-X or in SRC-Y) by ± 4 mm along the horizontal direction, and takes the maximum of the 4.

Baffle	BS aperture	SRM3 aperture	Common mode rejection
no baffle	37cm	26.5cm	174ppm
	37cm	34cm	177ppm
	40cm	26.5cm	6ppm
	40cm	34cm	3ppm
21 cm x 26cm	37cm	26.5cm	60ppm
21 cm x 26cm : 4mm x offset			220ppm
22cm x 26cm			140ppm
22cm x 26cm : 4mm x offset			180ppm
22cm x 22cm			140ppm
26cm x 26cm			170ppm

When the displacement is within 2mm, very small changes were observed. The difference between this calculation and the previous one based on the contrast defect will come from the fact that the

00 mode signal is mainly determined by the central region of the field, while the contrast defect comes from the difference in the peripheral region. The common mode rejection calculation assumes that the output mode cleaner picks up the 00 signal correctly and the local oscillator CR is clean to pickup correct 00 signal sideband.

7. Summary

Based on the simulation of fields in coupled cavities consisted of PRC / SRC and X / Y arm with a BS in between, the optimal shape of the baffle was calculated to be an oval shape with axis sizes 21cm in the horizontal direction and 26cm in the vertical direction.

By placing same shape baffles around the BS facing to the x arm and to the y arm, the contrast defect is reduced by factor of 5 without losing the signal sideband. Common mode rejection improves by factor 3, from 170ppm to 60ppm.

The requirement of the placement accuracy needs to be determined by properly interpreting the effect of the baffle offset.

8. References

1. H. Yamamoto, "SIS (Stationary Interferometer Simulation) manual", LIGO-T070039